Institute of Physics Publishing Journal of Physics: Conference Series **32** (2006) 167–179
doi:10.1088/1742-6596/32/1/026 Sixth Edoardo Amaldi Conference on Gravitational Waves

Grating Angle Magnification Enhanced Angular and Integrated Sensors for LISA Applications

Ke-Xun Sun*, Saps Buchman, and Robert Byer

Hansen Experimental Physics Laboratory, Stanford University, CA 94305-4085, USA
*kxsun@stanford.edu, tel: 650-736-1056

Short Title: "Grating Angle Magnification Enhanced Sensors"

PACS number: 04.80.Nn, 95.55.Ym, 07.60.Ly, 42.79.Dj, 42.40.Eq, 42.79.-f

Keywords: Grating, Angle Magnification, Angular Sensor, Integrated Sensor, Gravitational Wave Detection, LISA, BBO

Presented at "Amaldi6", Poster No. 72, Space Detector Session
6th Edoardo Almadi Conference on Gravitational Waves
Bankoku Shinryoukan, Kise Nago, Okinawa, Japan
June 20-24, 2005

Abstract

The Laser Interferometer Space Antenna (LISA) and the Big Bang Observer (BBO) require angular sensing in their gravitational reference sensor (GRS), telescope pointing, and spacecraft control. The conventional angular sensing schemes utilize simple geometric reflections as the sensing mechanism.

We propose and demonstrate the use of grating diffraction orders as angular sensing signal beams. The grating angular sensor can be far more sensitive than a simple reflection scheme for two reasons. First, the diffractive angles can vary more than the incident angle when the grating rotates. The grating thus magnifies the variation of the input angle. Second, the cross section of the diffracted beam is compressed by the oblique projection, resulting in a higher energy density. These two favorable effects become more pronounce for a normal incidence beam to diffract at grazing angles. We have conducted a preliminary experiment and demonstrated an angular sensitivity below 10 nanoradians per root hertz over a short working distance, meeting the Space Technology 7 (ST-7) GRS and LISA requirements for proof mass angular sensing.

Our proposed grating-based angular measurement does not introduce additional optical elements between the sensed surface and the photodiode. Thus, it eliminates measurement uncertainty due to in-path optics. The proposed grating sensor can be generalized to build an integrated sensor for both angular and displacement sensing.

1. Introduction

High precision angular sensing plays an important role in LISA and BBO, as well as their pilot flight ST-7 and LISA Pathfinder Package (LTP) [1-5]. Proof mass orientation, telescope steering, and spacecraft flight control are some examples requiring angular sensing and control. The precision required for proof mass angular orientation measurement is ~0.1 μrad $Hz^{-1/2}$, and for telescope steering, ~1 nrad/$Hz^{1/2}$. Angular sensing is also widely used in the ground-based LIGO for interferometer control.

Conventional optical angular sensors rely on deflection by simple geometric reflection from the object. To enhance the angular sensitivity, one needs to increase the working distance from the sensed surface to the photodetector. However, this approach is difficult to implement in the space-borne gravitational reference sensor (GRS), due to the compactness and stability requirements of a LISA-class instrument. At limited working distances, the simple geometric reflection scheme may not have adequate angular sensitivity [6]. Interferometric sensing can be used to enhance angular sensitivity, at the expense of additional complexity in optics and detection. The added in-path optics components introduce angular noises due to mechanical and thermal variations, which are more pronounced at the lower frequencies in the LISA signal band. Our recent experiments [7] have demonstrated that a longer optical path is responsible for a higher noise floor level at low frequencies. It is desirable to enhance angular sensing sensitivity without lengthening the working distance.

The current geometry of LISA/ST-7 GRS presents unique challenges in configuring high precision angular sensors. The proof mass is enclosed in the housing shield with limited clear optical access. The gap between the proof mass and the housing wall is narrow, ~2 mm for ST-7 and 3 or 4 mm for LTP. Optical angular sensors with multiple reflections between the proof mass and the housing were designed for LTP [8]. However, this complicated arrangement is sensitive to housing shape changes due to environmental effects. Its sensitivity is about the same as the sensors based on simple geometric reflection.

We propose a novel angular sensor using a diffraction grating. This method has higher sensitivity thanks to the grating angle magnification and the beam cross-section compression. With proper data processing, information about pure rotation and pure displacement can be obtained. The grating angular sensor is all reflective, and it introduces no additional in-path transmissive optics. Any uncertainty produced by the extra optics is therefore eliminated. We have conducted a proof of principle experiment, and have demonstrated 10 nrad/$Hz^{-1/2}$ angular sensitivity over a mere 5 cm working distance.

2. Grating angular magnification enhanced angular sensor

A grating is a wave front segmenting and diffracting device. Diffraction orders are formed by coherent addition of the multiple re-diffracted wavefront segments. Gratings have been used in optics mostly for spectral sensitive applications. Recently we

have extended the grating application into interferometry using its kinetic properties previously less explored. We investigated the all-reflective, grating-based interferometers for high precision measurement for ground-based gravitational wave detection in 1996. All-reflective Michelson, Sagnac, and Fabry-Perot interferometers based on grating beam splitters were demonstrated [9]. We proposed using Fabry-Perot grating cavities as a displacement sensor for GRS [10]. We have shown that a grating splitter can significantly simplify LISA external interferometry [10].

Figure 1 shows the fundamental property of the grating diffraction orders. For a laser beam of wavelength λ incident onto the grating, the output angle θ_m of the m-th diffraction order is given by the grating equation,

$$d(\sin\theta_m - \sin\theta_{inc}) = m\lambda, \tag{1}$$

where θ_{inc} is the incident angle, and d is the grating period.

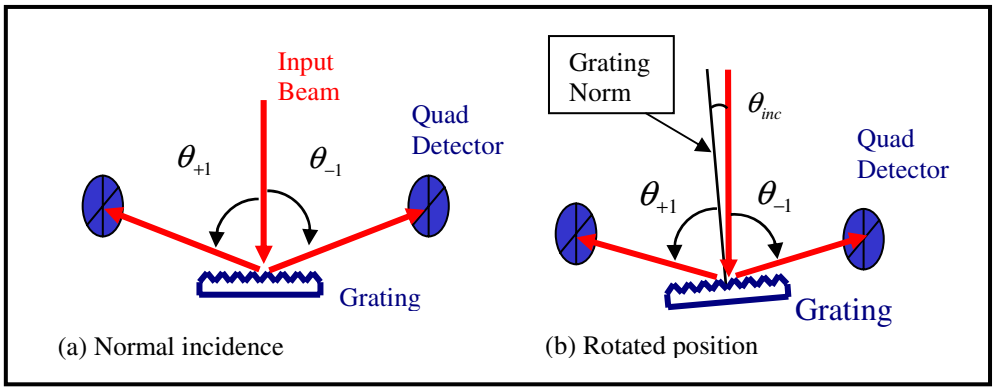

Figure 1. The diffractive orders from one-dimensional grating functions as angular sensing beams. (a) Normal incidence for the non-rotated case. (b) Oblique incidence for the rotated case

We propose putting a grating or a diffractive optics pattern on the surface of the proof mass, and using the motion of the diffracted beams for angular sensing. The shape of the proof mass can be faceted or spherical. There are several ways to put a grating onto the proof mass, such as electron beam lithography, diamond machining, and mechanical imprinting. A gold coating could be applied for lower loss. The grating needs only a small area to diffract a narrowly collimated laser beam with a diameter smaller than 1 mm. For a practical numerical value at wavelength 1064 nm, a Rayleigh range of 100 mm only requires a beam diameter of ~0.06 mm. The proof mass may move in a confined range, which is smaller than the 30 μm in ST7 and LISA designs. Thus, 1 mm diameter active grating area should be sufficient to cover the mechanical dynamic range. A fixed mark on the proof mass provides unambiguous determination of proof mass position and orientation.

Patch effect [11], or surface potential variation, may be of concern. However, it is estimated that the possible increase in patch effect is negligible for such a small area bearing a shallow corrugation with depth less than 30% of the laser wavelength, as the patch effect is roughly proportional to total surface area.

Grating angle magnification is an interesting property that has not been previously explored as a method of sensitivity enhancement for angular sensors. We show that angle magnification enables a grating rotational sensor to achieve substantial improvement in measurement precision over plane mirror reflection. When the grating rotates by an angle $\Delta\theta_{inc}$, the m-th diffraction order pointing will change by $\Delta\theta_{m}$, which is determined by,

$$\cos(\theta_m)\Delta\theta_m = \cos(\theta_{inc})\Delta\theta_{inc} \qquad \text{or,} \quad \Delta\theta_m = \left(\frac{\cos(\theta_{inc})}{\cos(\theta_m)}\right)\Delta\theta_{inc} \ . \tag{2}$$

When θ_{inc} is small, i.e. near zero, and θ_m is large, i.e. near 90°, the m-th diffraction order output incremental angle $\Delta\theta_m$ can be substantially larger than the rotational angle $\Delta\theta_{inc}$. If $\theta_{inc} = 0$ and $\theta_m = 80°$, then $\Delta\theta_m \approx 5.8\Delta\theta_{inc}$. The signal is thus enhanced without any other complication such as increasing laser power.

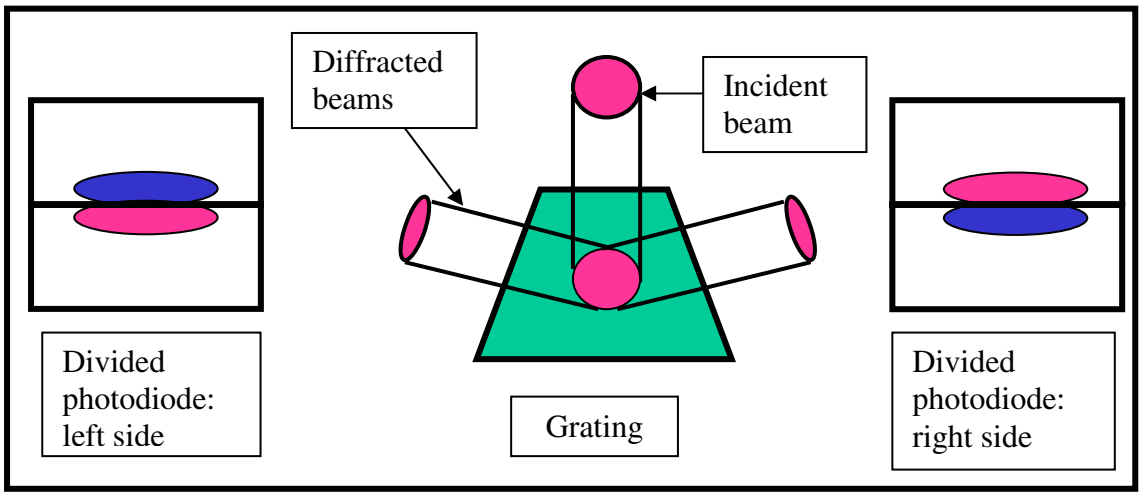

Figure 2. The projected beams at larger diffraction angles have smaller cross sections, higher energy densities, and will produce higher differential currents from a divided photodiode.

Further enhancement of the sensitivity comes from the beam size compression in the angular movement dimension as the result of oblique projection. Figure 2 illustrates the situation when a divided photodiode is used to detect beam movement. When the beam cross section is compressed, the energy density becomes higher. Therefore, the same beam movement induces a greater percentage differential energy variation between the two sides of the divided photodiode. When the beam straddles the middle of the binary detector, the signal variation of the differential photocurrent is increased by a

factor equal to the ratio of energy densities of the two beams, $\left[\cos(\theta_{inc})/\cos(\theta_{\pm 1})\right]$, where for definiteness we have used 1 order.

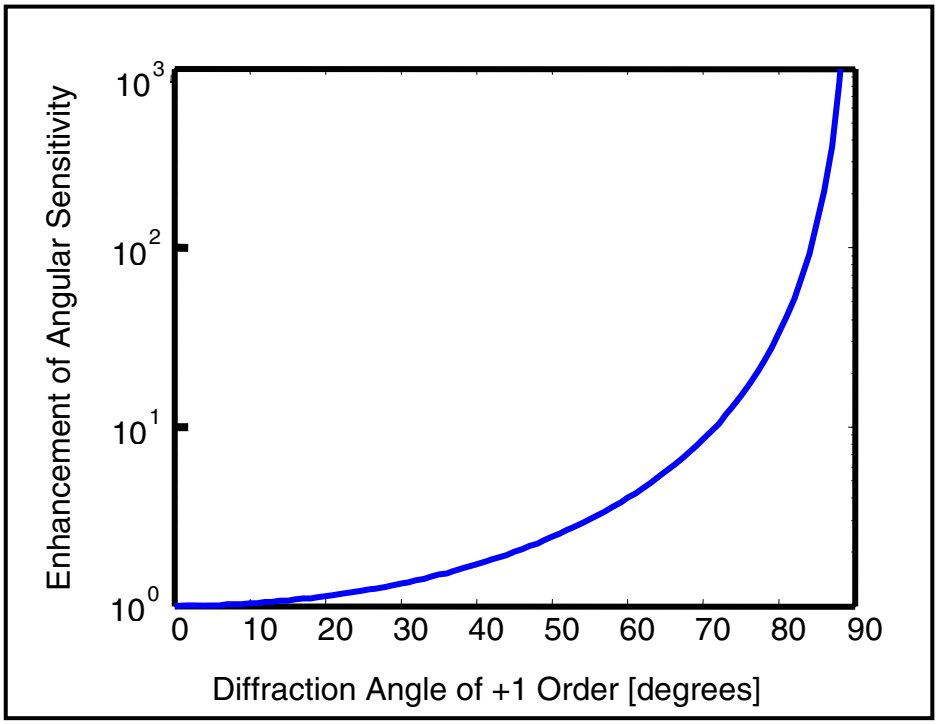

Figure 3. The enhancement factor for angular sensitivity using a grating sensor. K = 1 is assumed. Observe the large enhancement in angular sensitivity at grazing angles.

Combining these two magnifying effects, the total enhancement in sensitivity due to the grating becomes,

$$G_{grat} = K\left(\frac{\cos(\theta_{inc})}{\cos(\theta_{\pm 1})}\right)^2, \tag{3}$$

where K is a constant that depends on the sensor system configurations that are compared. If the simple reflection system utilizes 100% of its input light, and the grating sensing system uses both diffraction orders, then $K = (\eta_{+1} + \eta_{-1})/1$, where η_{+1}, and η_{-1} are the diffraction efficiencies for the +1 and –1 orders respectively. If the simple reflection system has a 50/50 beam splitter, as does our experimental system in an earlier effort for ST-7 metrology, the quad detector only collects 50% of the input light. Then $K = (\eta_{+1} + \eta_{-1})/0.5$, which leads to $K > 1$, where we have made the realistic assumption that $\eta_{+1} = \eta_{-1} \approx 0.3$. For a resonantly enhanced grating system, as we will describe in the next section, all input light can pass onto the pair of the quad detectors. This leads an

even more favorable $K = 2$. For simplicity, we use $K = 1$ in what follows. For $\theta_{inc} = 0°$ and $\theta_{+1} = 80°$, G_{grat} 33. For $\theta_{+1} = 85°$, G_{grat} 67. Figure 3 is semilog plot of equation (3) assuming $K = 1$. Evidently there is a large gain in angular sensitivity when the diffraction approaches a grazing angle.

By proper choice of the grating period *d,* we can design the grating to have only 0, +1 and –1 diffraction orders for a symmetric angular sensor, thus avoiding energy loss to higher diffraction orders. For the LISA and ST-7 GRS, large diffraction angles θ_1 are a natural choice, since the diffracted beams can pass through the gap between the proof mass and surrounding wall to illuminate the quad detector mounted near the corners of the housing walls. The light access openings do not reduce the capacitive sensing areas, and the light beams do not interfere with electrostatic forcing. Figure 4 illustrates the configuration.

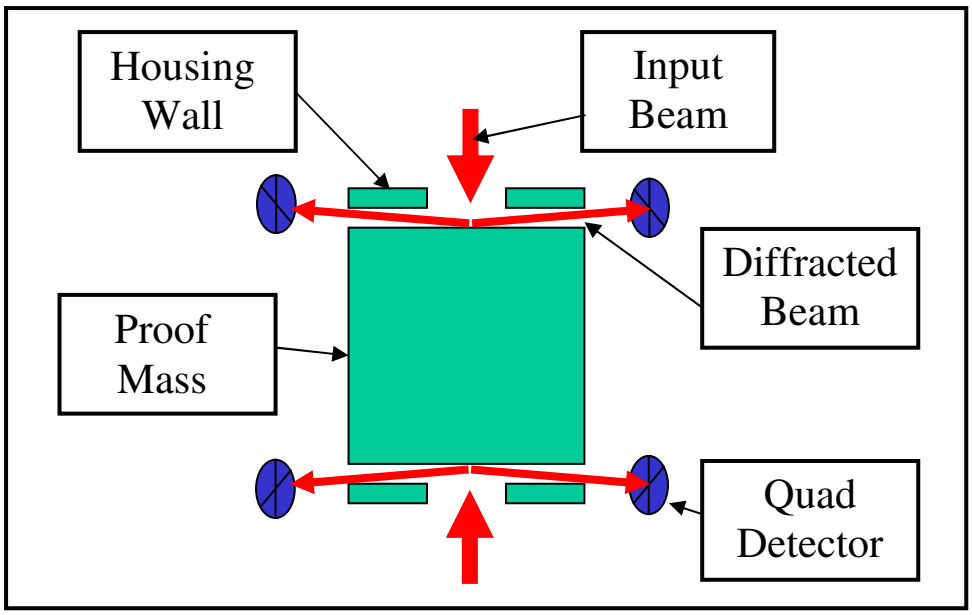

Figure 4. A possible implementation of the grating angular sensor for LISA GRS configurations. The diffracted beams pass through the gap between the proof mass and the housing at a grazing angle.

The angular sensing system is all-reflective, eliminating the measurement uncertainty introduced by in-path optics that could affect beam pointing. For example polarization beam splitters that are often used in more traditional angular sensing systems may be made from two pieces of glass glued together. The instability of such a beam splitter during flight could incur risks. The temperature variation induced refractive index change (dn/dT effect) is another concern.

It is advantageous to use two symmetrically placed quad detectors on opposite edges of the grating. One reason is that the proof mass can have both angular and

displacement motion, and both can produce output from a detector. The pure rotational signal can be obtained by subtracting the two differential outputs from the two quad detectors. Therefore the two-detector scheme provides a basis for proper signal processing. Higher sensitivity is also obtained, since the rotational signal is doubled. The pure displacement signal is obtained by adding the two differential outputs from the two quad detectors. Using two quad detectors also adds redundancy and reliability. The angular signal component is typically much larger than the displacement component, thanks to the grating angle magnification. In addition, the displacement information is also available from other measurements. Therefore, considerable sensing functionality is maintained even when there is only one detector.

3. Integrated angular and displacement sensor and two-dimensional grating sensor

Figure 5 illustrates a design for an integrated angular and displacement grating sensor. First, the one-dimensional grating based angular sensor can be generalized to a two-dimensional grating. The two dimensional grating consists of sets of grooves, typically in orthogonal directions. The grating equation Eq. (1) can be generalized to handle two-dimensional gratings by designating the different groups of grating periods, diffractive orders, and diffraction angles [12]. The two-dimensional grating can be fabricated using similar techniques as those used for the one-dimensional grating. Two-dimensional grating enables sensing rotations about both the X- and Y-axes with enhanced sensitivity. If quad detectors are used, this scheme can also detect rotation about the Z-axis, but without sensitivity enhancement.

The 0^{th} order reflected back from the grating can be used for displacement measurement. By adding a Littrow mounted grating along the Z-axis, as shown in Figure 5, a resonant cavity is formed between the grating and the proof mass surface. The interferometric cavity fringe can be used for a high sensitivity measurement of the displacement between the proof mass front surface and the Littrow grating [9, 10]. An RF technique can be added to aid the absolute distance measurement. The measurement using a resonant cavity does not require an extra reference surface and associated path length. It therefore simplifies the GRS architecture. In a transmissive optics version, the Littrow mounted grating can be replaced with a coupler with a finite reflectivity.

The resonant cavity allows for an impedance-matched design. Namely, the total zeroth order diffraction efficiency of the Littrow mounted grating is equal to the reflection of the zeroth order from the 2-dimensional grating. Then all of the input light will transmit through the cavity and be received by the photodetectors if the scattering losses are negligible. The summation of all photocurrents will indicate the change in the cavity length. The differential currents and their combination will reflect the angular motion of the proof mass. Thus, the configuration in Figure 5 can measure all three rotational degrees of freedom and the displacement along the Z-axis. For even more complete redundancy and also for balance of radiation pressure, a similar configuration can be implemented at the back surface of the proof mass.

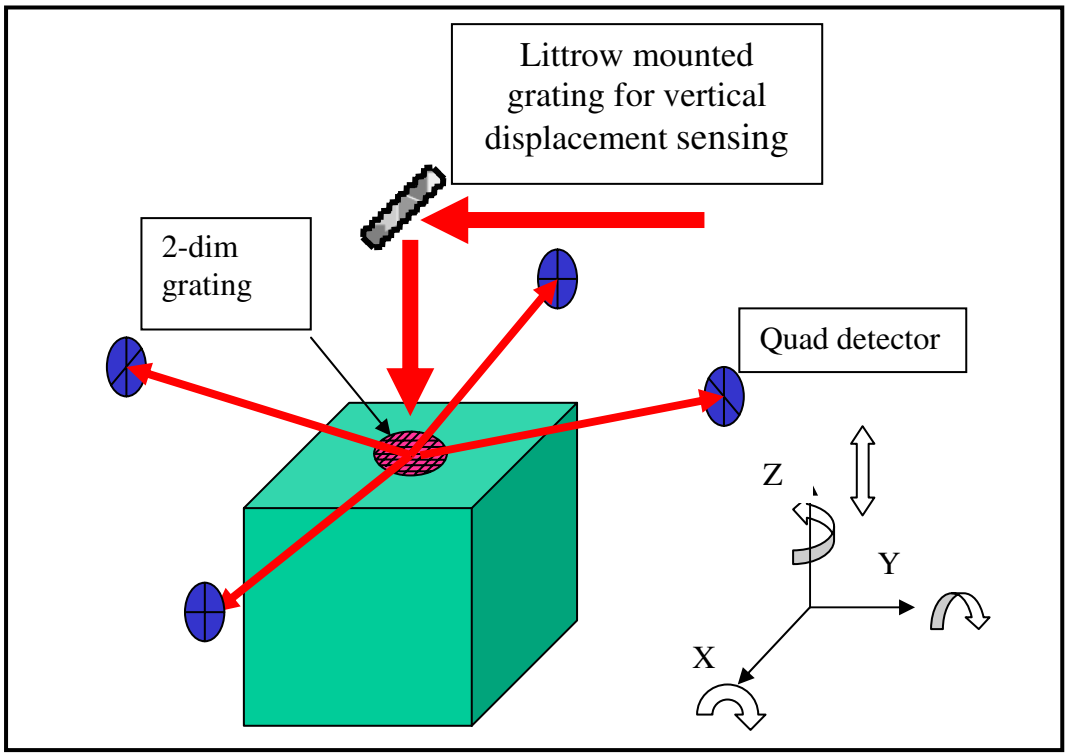

Figure 5. Integrated, all-reflective angular and displacement sensor orders. The two-dimensional grating on the proof mass still functions as a supplier of angular sensing beams. A Littrow-mounted grating is added to form a displacement sensor using grating cavity resonance. The integrated sensor can measure all three rotational angles, and measure the displacement with higher sensitivity in the Z-direction.

This grating sensor design provides a high performance, integrated angular and displacement senor for the GRS. The all-reflective, diffractive optics architecture is simple and robust compared with capacitive sensing. It has a large amount of redundancy built-in, leading to higher reliability. It has significantly lower back action that can disturb the proof mass.

Of particular note, LISA has recently changed [13] its baseline design to a non-direct illumination architecture, which has been proposed in detail in 2004 [10]. The grating sensor design described here can be used to simplify the implementation of the stand-alone or modular GRS. The Z-axis can be taken as the sensitive direction, and the Littrow grating can be used to couple the precision measurement. The proposed all-reflective configurations do not need any additional references, thus simplify the implementation of the non-direct illumination scheme.

4. Experiment

We have conducted a preliminary experiment to demonstrate the key features of grating angular sensor. Figure 6 shows the experimental setup. A Nd:YAG NPRO laser with a wavelength of 1064 nm was used as the light source. For normal incidence, first order diffraction at grazing angles of 81° would require a groove density of ~926 lines/mm, which demanded a custom built order. Therefore, for a proof-of-principle demonstration, an off-the-shelf gold-coated grating with a groove density of 1200 lines/mm was used. The laser beam was introduced to the grating an incident angle of 16.8°, which produced the –1 order at 81° on the same side of the grating norm. The diffraction efficiency for the –1 order was ~45%. The zeroth order was symmetric with the input beam on the other side of the grating norm, providing an indicator of the movement of simple geometric reflection. There were no other diffraction orders, thanks to the choices of the input angle and the density of grating grooves. The grating could be coarsely rotated by the mechanical mount. The fine rotation of the grating was realized by driving a pair of piezoelectric transducers (PZT) mounted symmetrically about the grating center in the horizontal plane. The grating could be driven in either pure displacement motion by applying oscillating voltages with the same phase to both PZTs, or in pure rotational motion by applying oscillating voltages with opposite phases.

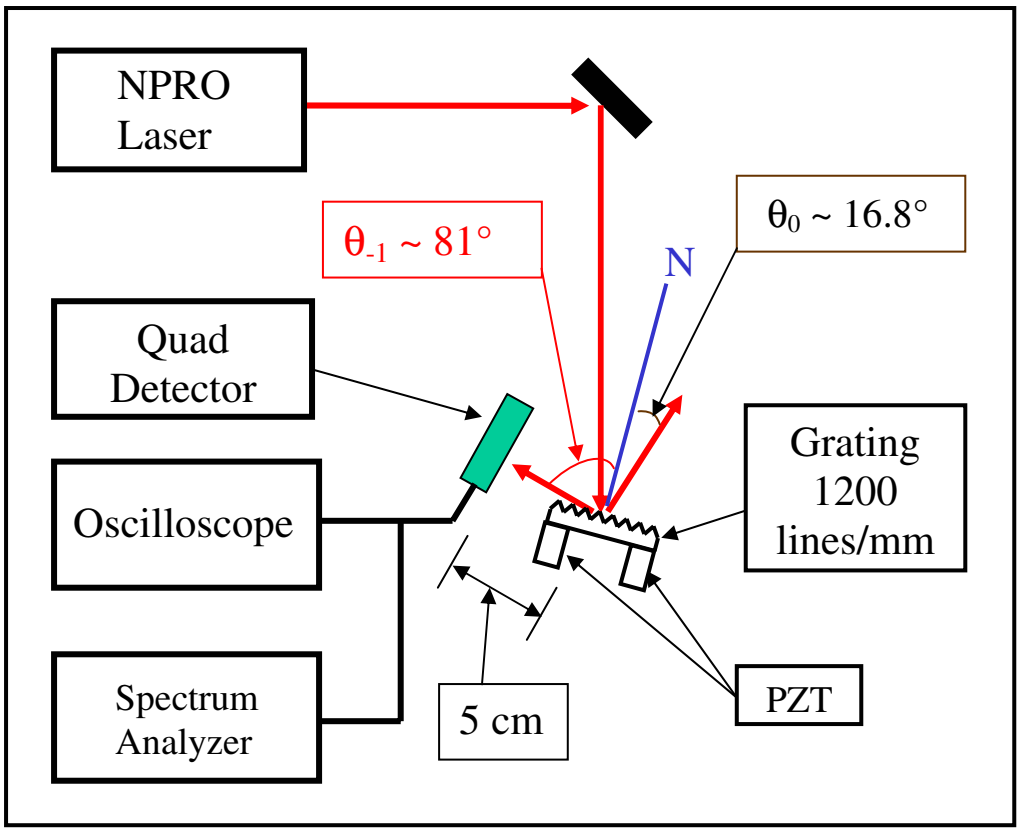

Figure 6. Experimental setup. "N" represents the norm to grating surface. The detector for 0th order diffraction is omitted in this schematic.

According to equation (3), the gain in angular sensitivity for this particular experiment is $\left(\cos(16.8^{o})/\cos(81^{o})\right)^{2} \approx 38,$ for $K = 1$, and approximately 17 for $K = 0.45$, if we take the total diffraction efficiency as the value of K.

The grating angle magnification effect was easily observed and measured by rotating the grating and monitoring the movement of the 0^{th} and -1 order beam spots on thermal cards at a distance ~30 cm away. The result agreed with the calculation shown in equations (1) and (2). The beam compression effect was confirmed using a CCD beam profiler to image the input and the –1 order diffracted beam cross sections..

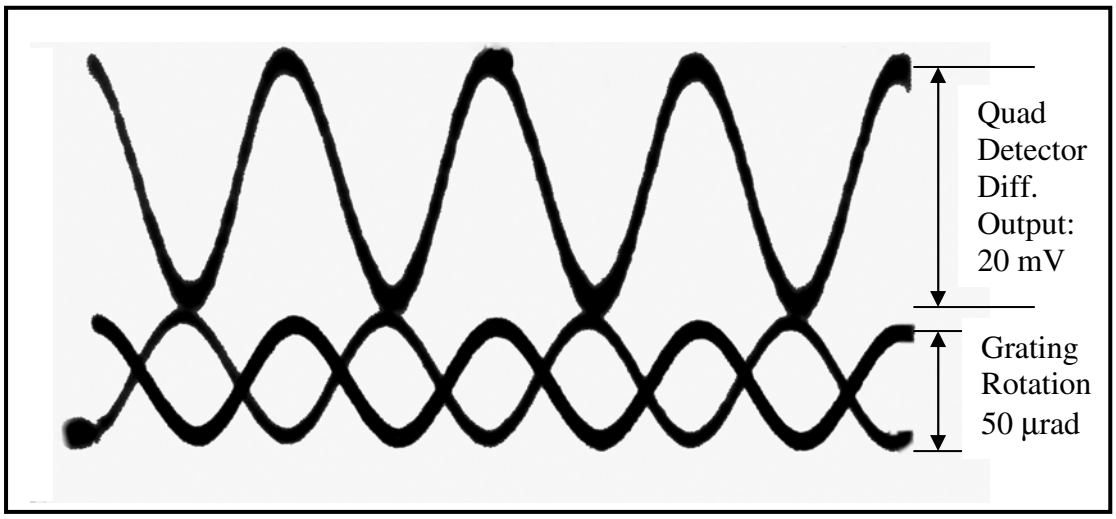

Figure 7. Oscilloscope traces for the grating angular sensor. Top trace: the differential output from the left and right halves of the quad detector. The amplitude was 20 mV. The bottom traces: PZT driving voltages with opposite phases, the equivalent rotational angle produced by the differential voltage was 50 μrad. The frequency of oscillation was 1 kHz.

For the sensitivity measurement, a quad detector was placed 5 cm away from the illumination area of the grating to measure the angular movement of the –1 diffraction order. This short working distance was deliberately chosen to emulate the working environment of the realistic GRS. The differential voltage between the left and right halves of the quad detector was monitored as the signal. An oscilloscope was used to directly observe the waveform, and an FFT spectrum analyzer was used for the sensitivity measurement at finer rotation angles. Figure 7 shows the oscilloscope trace of the differential output when the PZT was driven by a pair of voltages at 1 kHz with opposite phases. Based on the PZT calibration, the equivalent rotational angle was approximately 50 μrad. The quad detector output signal amplitude was 20 mV.

To determine the angular sensitivity of the grating angular sensor, PZT driving voltages were reduced to 1% of that in Figure 6. The amplitude of the rotation angle for the lower drive was only 0.5 μrad. Figure 8 (a) shows the FFT signal analyzer observation. The signal to noise ratio was recorded to be 38~40 dB at an equivalent

bandwidth of 100 Hz. In this preliminary experiment, there were measurement uncertainties, mostly related to the readout precision. Due to the wide noise floor, the PZT driving voltage was kept relatively high to exhibit the height of the spectral peak, and therefore the readout resolution is limited. The per trace variation of the spectrum is ~0.25 division. The FFT spectrum analyzer is mostly calibrated at the upper readout section due to the range of the available signal generator. Therefore, we have used a conservative 34 dB peak height to calculate the noise floor, and used 3σ value for 95% confidence. Taking into account all these factors, a conservative estimate of the noise floor was ~5 nrad/$Hz^{1/2}$. The angular sensitivity of the grating angular sensor at 3 dB signal-to-noise ratio is therefore ~10 nrad/$Hz^{1/2}$. We are working towards a two-detector system and improving the sensitivity measurements and calibration.

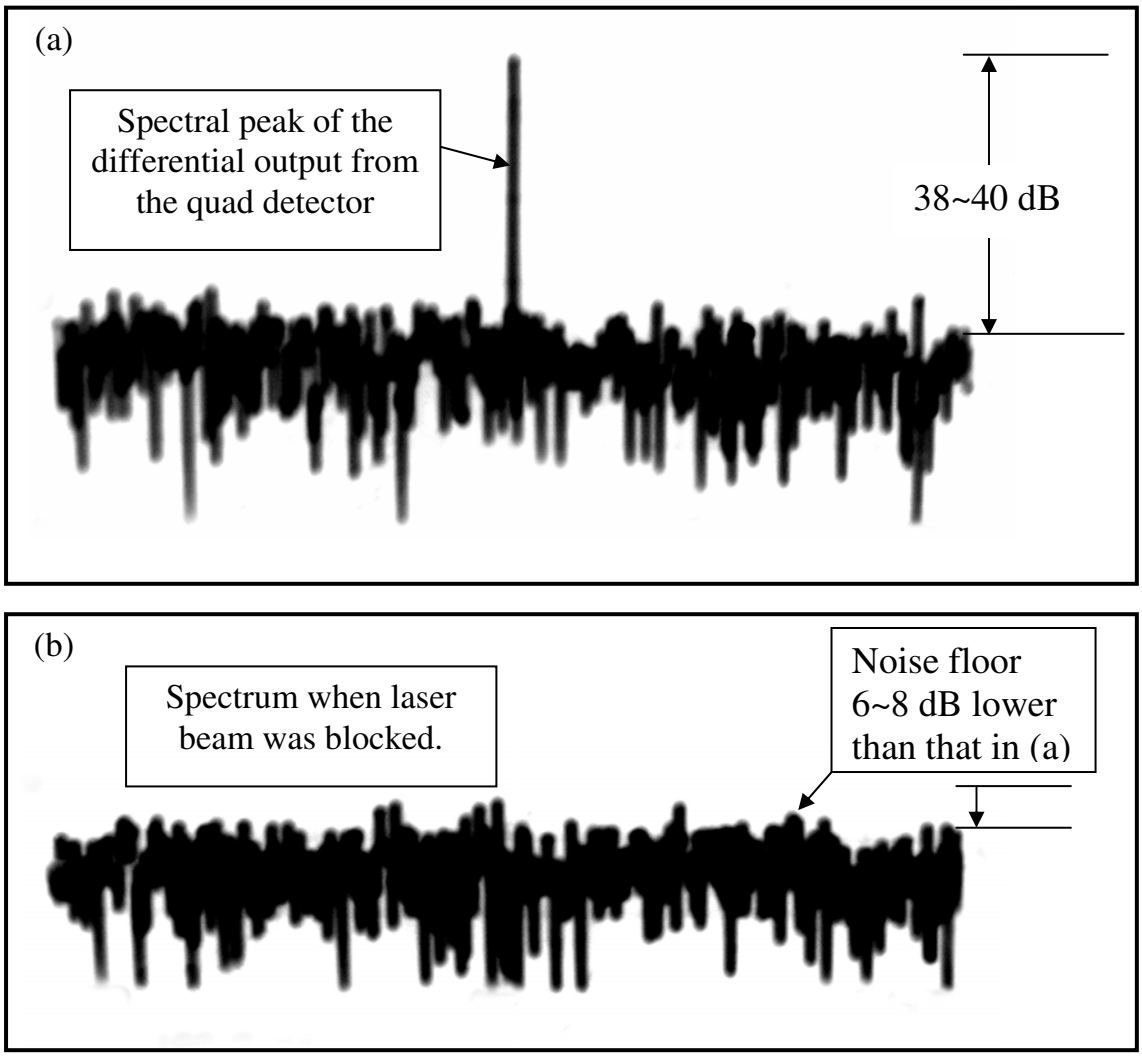

Figure 8. (a) Spectrum of the differential output of the quad detector in the grating angular sensor. The equivalent angular rotation amplitude was 0.5 μrad, driven by PZT voltages of 2V, or 1% of that in Fig. 7. The frequency of oscillation was 1 kHz. (b) Laser spectrum when the laser beam was blocked. No leaked signal was observed.

Figure 8 (b) shows the spectrum when the laser was blocked while PZT driving voltages were kept at the same level as before. The absence of the signal peak proved that there was no electrical signal leaking into the optics and electronics measurement system. Meanwhile, the noise floor was observed to be lower by 6~8 dB, thanks to the lack of laser intensity noise. This suggested that further improvement in angular sensitivity would be possible by smoothing the laser intensity. Using the two-detector scheme would also suppress the intensity noise by subtracting the differential outputs from the two quad detectors. Experimentally, the sensitivity of the grating sensor has exceeded the ST-7 and LISA GRS specification of 0.1 $\mu rad/Hz^{-1/2}$.

5. Conclusion

We have proposed and experimentally demonstrated a novel grating angular sensor. The sensitivity of the grating angular sensor is enhanced by grating angle magnification and beam compression. A sensitivity level of 10 $nrad/Hz^{1/2}$ at a short working distance of 5 cm has been demonstrated in the preliminary experiment, meeting the ST-7 and LISA GRS requirements for both sensitivity and compactness. The grating angular sensor is all-reflective, immune to problems caused by in-path transmissive optics, and is thus expected to have better mechanical and thermal stability than a conventional angular sensor. Further, the grating angular sensor can be generalized to an integrated, all-reflective sensor for both displacement and angle sensing. Research efforts are underway to develop a two-detector system and related grating fabrication technologies. The grating sensor may also find applications in the LIGO interferometer control.

Acknowledgements

We thank Dr. Robert Spero at JPL for stimulating discussions. The bulk of the material in this paper was presented to the Jet Propulsion Laboratory (JPL) in October 2004 and March 2005 as a research proposal. We thank Professor Dan DeBra, John W. Conklin, and Patrick Lu at Stanford University for critical reading of the manuscript. The composition of this paper is supported by the JPL Director Research and Development Fund (DRDF) program and the National Science Foundation LIGO program.

References

[1] LISA Study Team, "LISA Pre Phase A Report, 2nd Edition"

[2] LISA science team, "System and technology report", ESA (2000)

[3] Sterl Phinney, Peter Bender, Saps Buchman, Robert Byer, Neil Cornish, Peter Fritschel, William Folkner, Stephen Merkowitz, Karsten Danzmann, Luciano DiFiore, Seiji Kawamura, Bernard Schutz, Alberto Vecchio, Stefano Vitale, "The Big Bang Observer"

[4] S. Buchman, B. Allard, G. Allen, R. Byer, W. Davis, D. DeBra, D. Gill, J. Hanson, G.M. Keiser, D. Lauben, I. Mukhar, N. A. Robertson, B. Shelef, K. Sun, S. Williams, *"The Stanford Gravitational Reference Sensor",* 5th International LISA Symposium, ESTEC, Noordwijk, The Netherlands, 12-16 July 2004

[5] R. Spero and A. Kuhnert, "The ST7 interferometer", Class. Quantum Grav. **21** (2004) S589–S595

[6] F. Sabur, presentation at Stanford University for DRDF review, September 2004

[7] G. Allen, W. Bencze, R. Byer, A. Dang, D. Lauben, S. Dorlybounxou, J. Hanson, S. Higuchi, K. Sun, L. Ho, G. Huffman, F. Sabur, K. Sun, R. Tavernetti, L. Rolih, R. Van Patten, J. Wallace, S. Williams, "Calibration and testing of the ST7 capacitive sensor using an optical interferometer with fiber optic input and output", Paper submitted Amaldi 6 Proceedings

[8] F Acernese, E Calloni, R De Rosa, L Di Fiore, L Garcia, and L Milano, "An optical readout system for the LISA gravitational **reference sensors" Class. Quantum Grav. 21 (2004) S621–S627**

[9] K.-X. Sun and R. L. Byer, "All-reflective Michelson, Sagnac, and Fabry-Perot interferometers based on grating beam splitters", Opt. Lett. **23**, 567 (1998).

[10] K-X. Sun, G. Allen, S. Buchman, D. DeBra, and R. L. Byer, "Advanced Architecture for High Precision Space Laser Interferometers ", 5th International LISA Symposium, ESTEC, Noordwijk, The Netherlands, 12-16 July 2004. See also, Classical and Quantum Gravity **22** S287-S296, (2005)

[11] C C Speake, "Forces and force gradients due to patch fields and contact-potential differences," Class. Quantum Grav. 13 (1996) A291–A297.

[12] J. W. Goodman, "Introduction to Fourier Optics", McGraw-Hill, New York, 1968.

[13] G. Heinzel, "The LISA Pathfinder", LISA interferometry section, Amaldi 6 website http://tamago.mtk.nao.ac.jp/amaldi6/06.spd/Wed0915_amaldi6_ltp.pdf